

# Phonon-mediated electron attraction in $\text{SrTiO}_3$ via the generalized Fröhlich and deformation potential mechanisms

Christopher J. N. Coveney,<sup>1</sup> Norm M. Tubman,<sup>2,\*</sup> Chih-En Hsu,<sup>3,4</sup> Andres Montoya-Castillo,<sup>5</sup> Marina R. Filip,<sup>1</sup> Jeffrey B. Neaton,<sup>6,7,8</sup> Zhenglu Li,<sup>4</sup> Vojtech Vlcek,<sup>9,10</sup> and Antonios M. Alvertis<sup>11,†</sup>

<sup>1</sup>*Department of Physics, University of Oxford, Oxford OX1 3PJ, United Kingdom*

<sup>2</sup>*NASA Ames Research Center, Moffett Field, California 94035, United States*

<sup>3</sup>*Department of Physics, Tamkang University, New Taipei City 251301, Taiwan*

<sup>4</sup>*Mork Family Department of Chemical Engineering and Materials Science, University of Southern California, Los Angeles, California 90089, USA*

<sup>5</sup>*Department of Chemistry, University of Colorado Boulder, Boulder, CO 80309, USA*

<sup>6</sup>*Materials Sciences Division, Lawrence Berkeley National Laboratory, Berkeley, California 94720, United States*

<sup>7</sup>*Department of Physics, University of California Berkeley, Berkeley, California 94720, United States*

<sup>8</sup>*Kavli Energy NanoScience Institute at Berkeley, Berkeley, California 94720, United States*

<sup>9</sup>*Department of Chemistry and Biochemistry, University of California, Santa Barbara, CA 93106, USA*

<sup>10</sup>*Materials Department, University of California, Santa Barbara, CA 93106-9510, USA*

<sup>11</sup>*KBR, Inc., NASA Ames Research Center, Moffett Field, California 94035, United States*

(Dated: May 13, 2025)

Superconductivity in doped  $\text{SrTiO}_3$  was discovered in 1964, the first superconducting transition observed in a doped semiconductor. However, the mechanism of electron pairing in  $\text{SrTiO}_3$  remains a subject of debate. By developing a theoretical framework to incorporate dynamical lattice screening in the electronic Coulomb interactions of semiconductors and insulators, we demonstrate analytically that linear long-range coupling of electrons to multiple longitudinal optical phonons, described by a generalized Fröhlich mechanism, can result in superconductivity in  $\text{SrTiO}_3$ . Moreover, by combining our theory with first-principles calculations, we reveal an additional attractive interaction between electrons in  $\text{SrTiO}_3$  due to the deformation potential mechanism, arising from the mixed ionic-covalent character of the Ti-O bond. Our results may have implications for the emergence of phonon-mediated electron attraction and superconductivity in a broad range of materials.

The prediction that doped semiconductors can exhibit phonon-mediated superconductivity was made in 1964 in the seminal works by Cohen [1, 2], leading to the discovery of superconductivity in doped  $\text{SrTiO}_3$  in the same year [3]. Since then, superconductivity has been discovered in several semiconductors, including  $\text{GeTe}$  [4, 5],  $\text{SnTe}$  [6, 7], and  $\text{MoS}_2$  [8]. Moreover, interfaces of  $\text{SrTiO}_3$  with  $\text{LaAlO}_3$  and  $\text{LaTiO}_3$  exhibit superconductivity [9–11], generating interest in interface engineering to design high-temperature superconductors. Therefore, understanding the mechanism of  $\text{SrTiO}_3$  superconductivity is key towards designing new types of superconductors.

To date, the precise mechanism of the pairing between electrons in  $\text{SrTiO}_3$  remains elusive. As  $\text{SrTiO}_3$  exhibits strong electron-phonon coupling [12, 13], several works have investigated the possibility of phonon-mediated superconductivity [1, 14–19]. Proposed mechanisms include inter-valley scattering [1, 14], coupling to polar [15], and defect [16] phonons, higher-order electron-phonon interactions [17], coupling to the soft infrared active zone-center phonon of  $\text{SrTiO}_3$  [18], which is enhanced by anharmonic damping [20], and Rashba coupling [19, 21]. However, the emergence of superconductivity through these mechanisms generally depends on parameters that are challenging to compute from first principles or to ac-

curately infer from experiment [22, 23]. A fully first-principles explanation for the phonon-mediated electron-electron attraction remains elusive, as  $\text{SrTiO}_3$  becomes superconducting at low doping densities where the Fermi energy is much smaller than the phonon frequencies, placing it in the non-adiabatic limit. As a result, the widely used Migdal-Eliashberg framework for phonon-mediated superconductivity does not apply [24], leading to an ongoing debate on the mechanism of Cooper pair formation.

Here we present a theory that rigorously incorporates lattice screening in electron-electron interactions. Without relying on adjustable parameters, we analytically demonstrate that lattice screening from multiple longitudinal optical (LO) phonons yields long-range attraction and superconductivity in  $\text{SrTiO}_3$ , in good agreement with experiments. Moreover, we translate our theory to a first-principles computational scheme, and show that the deformation potential associated with vibrations of the Ti-O bond provides an additional short-range attractive contribution to electron-electron interactions. Our theory, outlined in detail in our companion paper [25], applies to several doped semiconductors and insulators.

The density-density interaction between electronic states  $i, j$  is

$$U_{i\mathbf{R}j\mathbf{R}'}(\omega) = \int_V d\mathbf{r} \int_V d\mathbf{r}' \phi_{i\mathbf{R}}^*(\mathbf{r}) \phi_{i\mathbf{R}}(\mathbf{r}) W(\mathbf{r}, \mathbf{r}', \omega) \phi_{j\mathbf{R}'}^*(\mathbf{r}') \phi_{j\mathbf{R}'}(\mathbf{r}'). \quad (1)$$

\* [norman.m.tubman@nasa.gov](mailto:norman.m.tubman@nasa.gov)

† [antoniosmarkos.alvertis@nasa.gov](mailto:antoniosmarkos.alvertis@nasa.gov)

Here  $\phi_{i\mathbf{R}}(\mathbf{r})$  are a basis localized in real space, specifically maximally localized Wannier functions (MLWFs) [26] centered around lattice vectors  $\mathbf{R}, \mathbf{R}'$ . Additionally,  $W(\omega)$  is the frequency-dependent screened Coulomb interaction, which has two contributions: an electronically screened Coulomb interaction  $W^{el}$ , and a contribution from phonons. Within many-body perturbation theory and to the lowest order in the electron-phonon interaction, the phonon contribution to the screened Coulomb interaction is written as [27–29]

$$W^{ph}(\mathbf{r}, \mathbf{r}', \omega) = \sum_{\mathbf{q}, \nu} D_{\mathbf{q}, \nu}(\omega) g_{\mathbf{q}, \nu}(\mathbf{r}) g_{\mathbf{q}, \nu}^*(\mathbf{r}'). \quad (2)$$

Here  $D_{\mathbf{q}, \nu}(\omega)$  is the propagator of a phonon with branch index  $\nu$  at wavevector  $\mathbf{q}$ , and  $g_{\mathbf{q}, \nu}$  is the electron-phonon vertex. By inserting the overall screened Coulomb interaction  $W(\omega) = W^{el}(\omega) + W^{ph}(\omega)$  into eq. (1), we obtain the total interaction for electrons in states  $\phi_{i\mathbf{R}}, \phi_{j\mathbf{R}'}$  as  $U_{i\mathbf{R}j\mathbf{R}'}(\omega) = U_{i\mathbf{R}j\mathbf{R}'}^{el}(\omega) + U_{i\mathbf{R}j\mathbf{R}'}^{ph}(\omega)$ .

For the phonon-mediated interaction, as detailed in our companion paper [25], we obtain for periodic systems

$$\begin{aligned} U_{i\mathbf{R}j\mathbf{R}'}^{ph}(\omega) &= \langle \phi_{i\mathbf{R}} \phi_{j\mathbf{R}'} | W^{ph}(\omega) | \phi_{i\mathbf{R}} \phi_{j\mathbf{R}'} \rangle \\ &= \sum_{\mathbf{q}, \nu} g_{ii\mathbf{q}\nu}(\mathbf{0}) g_{jj\mathbf{q}\nu}^*(\mathbf{R}' - \mathbf{R}) \\ &\times \left[ \frac{1}{\omega - \omega_{\mathbf{q}, \nu} + i\delta} - \frac{1}{\omega + \omega_{\mathbf{q}, \nu} - i\delta} \right], \end{aligned} \quad (3)$$

where  $g_{mn\mathbf{q}\nu}(\mathbf{R}) = \langle \phi_{m\mathbf{R}} | g_{\mathbf{q}\nu} | \phi_{n\mathbf{R}} \rangle$ . Here we ignore non-local couplings of the form  $\langle \phi_{m\mathbf{R}} | g_{\mathbf{q}\nu} | \phi_{n\mathbf{R}'} \rangle$ , which are expected to be small in the Wannier representation. In the static limit, and for on-site ( $\mathbf{R} = \mathbf{R}'$ ) intra-band ( $i = j$ ) terms this becomes

$$U_{i\mathbf{R}i\mathbf{R}}^{ph, st} = -2 \sum_{\mathbf{q}\nu} \frac{|g_{ii\mathbf{q}\nu}(\mathbf{0})|^2}{\omega_{\mathbf{q}, \nu}}, \quad (4)$$

which is a purely attractive interaction, in agreement with the conventional understanding of the effect of phonon screening on electron-electron interactions [30]. The superscript “*st*” denotes the static limit  $\omega = 0$ .

In polar semiconductors and insulators, linear long-range dipolar electron-phonon coupling dominates the electron-phonon interaction [31], and is written as

$$\begin{aligned} g_{ij\mathbf{q}\nu}^{\mathcal{L}}(\mathbf{R}) &= i \frac{4\pi}{V} \sum_{\kappa} \left( \frac{1}{2NM_{\kappa}\omega_{\mathbf{q}, \nu}} \right)^{1/2} \frac{\mathbf{q} \cdot \mathbf{Z}_{\kappa} \cdot \mathbf{e}_{\kappa\nu}}{\mathbf{q} \cdot \epsilon_{\infty} \cdot \mathbf{q}} \\ &\times \langle \phi_{i\mathbf{R}}(\mathbf{r}) | e^{i\mathbf{q} \cdot \mathbf{r}} | \phi_{j\mathbf{R}}(\mathbf{r}) \rangle, \end{aligned} \quad (5)$$

which is the generalization of the Fröhlich model [32]. Here we ignore local field effects, *i.e.* we set  $\mathbf{q} + \mathbf{G} \rightarrow \mathbf{q}$ , where  $\mathbf{G}$  a reciprocal lattice vector. For an atom  $\kappa$ ,  $M_{\kappa}$  and  $\mathbf{Z}_{\kappa}$  are its mass and Born effective charge tensor respectively,  $\mathbf{e}_{\kappa\nu}$  a vibrational eigenvector, and  $\epsilon_{\infty}$  the dielectric matrix tensor.

By using the expression of eq. (5) in the phonon-

mediated electron-electron interaction of eq. (3), taking the static limit, and assuming an isotropic dielectric and dispersionless phonons, we obtain the expression

$$U_{\mathbf{R}\mathbf{R}'}^{ph, st, \mathcal{L}} = -\frac{\gamma^2}{\epsilon_{\infty} |\mathbf{R} - \mathbf{R}'|}, \quad (6)$$

where  $\gamma^2 = \sum_m \frac{\omega_{LO, m}^2 - \omega_{TO, m}^2}{\omega_{LO, m}^2}$ , and  $m$  runs over LO-TO phonon pairs of the system. This is an attractive interaction, with the contribution of each LO mode being proportional to the splitting  $\omega_{LO, m}^2 - \omega_{TO, m}^2$  from the corresponding transverse optical (TO) mode. This result is derived within our companion paper [25], alongside expressions for the general frequency-dependent case, which accounts for anisotropic dielectric and dispersive phonons. By comparing this expression to a repulsive electron-electron interaction  $1/(\epsilon_{\infty} |\mathbf{R} - \mathbf{R}'|)$ , it is evident that an overall long-range attraction appears when  $\gamma^2 > 1$ .

Superconductivity in SrTiO<sub>3</sub> emerges upon doping of the conduction bands, it is therefore critical to incorporate doped carriers into our theoretical framework in order to gain microscopic insights into this process. At low doping concentrations  $n$  below a critical Mott density  $n_c$ , doped carriers are localized and the system remains insulating, albeit with a modified dielectric constant. This can be estimated from a simple Lorentz-Lorenz model at the critical density as  $\bar{\epsilon}_{\infty} = \epsilon_{\infty} + 4\pi n_c \alpha$  [33], where the polarizability  $\alpha = 9(\epsilon_0/m^*)^{3/2}$  for a hydrogen-like defect. We compute using DFT/LDA and a *GW* correction of the band structure an electron effective mass of  $m^* = 0.39$ . The critical density is obtained via the Mott criterion  $n_c = 0.26 \left( \frac{m^*}{\epsilon_0} \right)^3 = 1.5 \times 10^{15} \text{ cm}^{-3}$ , in reasonable agreement with the experimental value of  $2 \times 10^{16} \text{ cm}^{-3}$  [34]. Beyond this critical density, an insulator to metal transition occurs, and doped carriers behave as free particles described by a Thomas-Fermi screening model. We thus generalize our expression of eq. (6) for the phonon-mediated electron-electron interaction to include screening from localized and free carriers, and in reciprocal space the total interaction becomes [15, 35]:

$$U_{\mathbf{k}\mathbf{k}'}^{st, \mathcal{L}} = \frac{4\pi}{\bar{\epsilon}_{\infty}} \cdot \frac{1 - \gamma^2}{|\mathbf{k} - \mathbf{k}'|^2 + \kappa_{TF}^2}, \quad (7)$$

where the Thomas-Fermi screening length  $\kappa_{TF}^2 = \frac{4m^* p_F}{\bar{\epsilon}_{\infty} \pi}$ , with the doping-dependent Fermi momentum  $p_F$  determined from the computed density of states. A more rigorous treatment of electron-phonon coupling incorporating doping is possible within a first-principles context [36].

For a single dominant LO phonon mediating the Coulomb interaction, Gor'kov derived an expression for the superconducting critical temperature in the non-adiabatic limit, where SrTiO<sub>3</sub> lies [15]. In Appendix B we generalize this using our expression for the Coulomb interaction incorporating long-range coupling to multiple

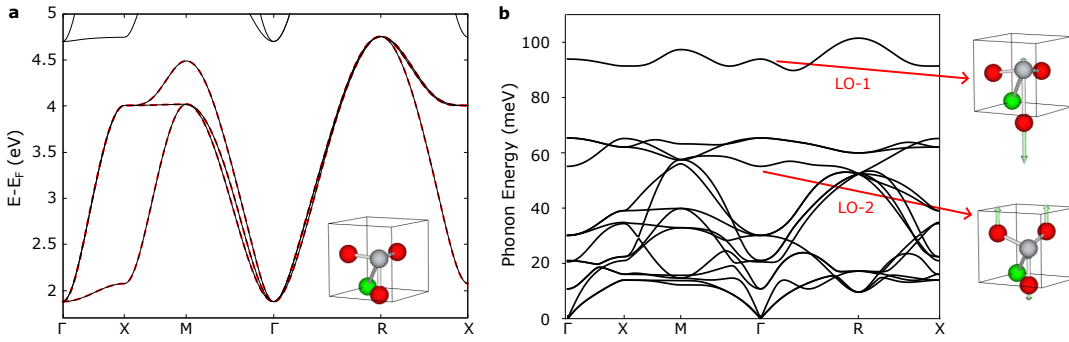


FIG. 1. Lowest conduction band manifold of  $\text{SrTiO}_3$  computed at the DFT-LDA level (black) and using Wannier interpolation (red) in panel **a** (energies relative to valence band maximum). The inset visualizes the unit cell of the system (Sr: green, Ti: gray, O: red). Panel **b** shows the phonon dispersion as obtained within DFPT including anharmonic corrections, alongside a visualization of the displacement patterns of the two highest frequency LO phonons.

$\epsilon_\infty$	$\epsilon_0$	$Z_{\text{Sr}}^*$	$Z_{\text{Ti}}^*$	$Z_{\text{O}}^{1*}$	$Z_{\text{O}}^{2*}$	$\omega_{\text{TO-1}}, \omega_{\text{LO-1}}$ (meV)	$\omega_{\text{TO-2}}, \omega_{\text{LO-2}}$ (meV)	$\omega_{\text{TO-3}}, \omega_{\text{LO-3}}$ (meV)
6.2	409	2.56	7.25	-5.69	-2.05	65, 94	21, 55	11, 21

TABLE I. DFPT results for  $\text{SrTiO}_3$ : high-and low-frequency dielectric constants  $\epsilon_\infty, \epsilon_0$ , Born effective charges of different atoms (along two directions for oxygen), and frequencies of the pairs of TO,LO modes at  $\Gamma$ , for the three IR active LO phonons.

longitudinal optical phonons and we obtain:

$$T_c = \frac{m^* \gamma}{\pi^3 \epsilon_\infty^2} x^2 \exp\left(-\frac{2x}{(\gamma^2 - 1) \ln(1+x)}\right), \quad (8)$$

where  $x = \pi p_F \bar{\epsilon}_\infty / m^*$ .

Above 105 K,  $\text{SrTiO}_3$  assumes a high-symmetry cubic perovskite structure, with perfectly aligned  $\text{TiO}_6$  octahedra. The unit cell in this phase, shown in Fig. 1a, consists of five atoms. Below 105 K the system is in its tetragonal paraelectric phase [37, 38], where the  $\text{TiO}_6$  octahedra undergo tilting, doubling the number of atoms in the unit cell. Here we focus on cubic  $\text{SrTiO}_3$  due to the qualitatively similar but simpler character of its phonons and electron-phonon coupling relative to the tetragonal phase. Fig. 1a shows the first three conduction bands of  $\text{SrTiO}_3$ , as obtained within density functional theory (DFT) and the local density approximation (LDA). Fig. 1b visualizes the  $\text{SrTiO}_3$  phonon dispersion, in excellent agreement with previous calculations [12, 39], as computed within density functional perturbation theory (DFPT), corrected for anharmonicity using finite differences, as outlined in Appendix A. The anharmonic correction is important, as for  $\text{SrTiO}_3$ , harmonic phonons computed at the LDA level of theory show instabilities at the  $R$  and  $M$  points in the Brillouin zone [40]. Table I summarizes the DFPT results for the dielectric constants, Born effective charges, and LO/TO mode frequencies of  $\text{SrTiO}_3$ . Cubic  $\text{SrTiO}_3$  has four LO phonons, three of which are IR active, and the frequencies of these are given in Table I. Additionally, Fig. 1b illustrates the displacement patterns of the two highest frequency LO modes, which involve vibrations of the Ti-O bond. In Appendix A we provide all computational details.

We now visualize in Fig. 2a the static long-range

phonon-mediated electron-electron interaction of cubic  $\text{SrTiO}_3$  in the undoped case, according to equation (6), and we compare to the long-range electronic repulsion  $U^{el} = 1/(\epsilon_\infty |\mathbf{R} - \mathbf{R}'|)$ . The phonon-mediated attraction (black) clearly overcomes the Coulomb repulsion (red) between electrons, resulting in a net attraction (blue). This results in the formation of Cooper pairs upon doping the conduction bands, and the critical temperature of superconductivity is visualized as a function of doping density in Figure 2b (black curve). We see that we reproduce the experimental dome-like behavior semi-quantitatively (experimental data are obtained from Refs. [14, 41]), although we generally overestimate the experimental  $T_c$ , and our predicted critical temperature is only accurate up to a factor of order one, as outlined in Appendix B. It is worth emphasizing that this result has been obtained by accounting for the linear long-range coupling to all LO phonons rigorously and on equal footing, and approximately incorporating doping in our Coulomb interaction of eq. (7). However, higher-order multi-phonon effects have been discussed to be important in  $\text{SrTiO}_3$  [39, 42], and specifically in the context of superconductivity [43–45]. In Appendix C we employ finite differences to estimate that on average, these effects can indeed be significant at higher temperatures, while at temperatures near 0 K they provide an effective reduction of  $g^2$  to 0.83 of its value when only accounting for linear electron-phonon coupling. The red curve in Figure 2b accounts for such a rescaling  $g^2 \rightarrow 0.83g^2$  from multi-phonon effects, bringing the predicted critical temperatures closer to experiment. Nevertheless, the qualitative behavior of the critical temperature, as a result of the linear coupling of electrons to multiple LO phonons, remains unchanged.

While the attractive interaction due to long-range electron-phonon coupling is sufficient to give rise to su-

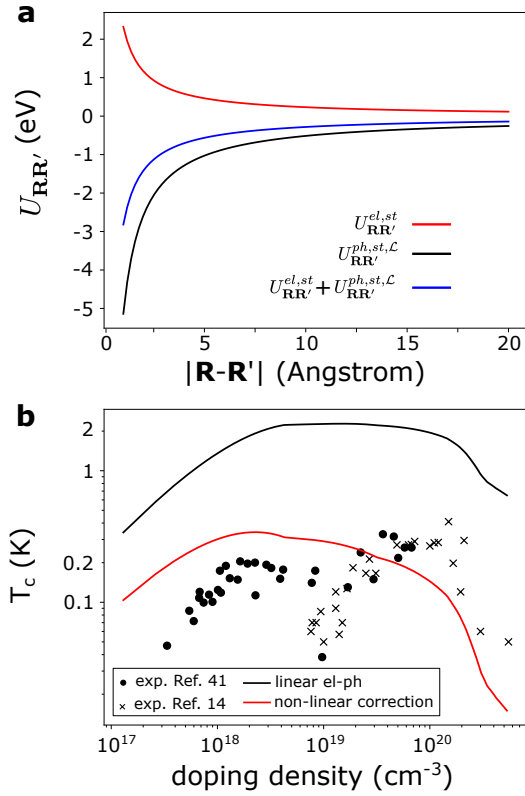


FIG. 2. Electron-electron Coulomb repulsion, phonon-mediated long-range electron attraction, and total interaction (panel a) as a function of distance between electrons. In panel b we visualize the superconducting critical temperature of SrTiO<sub>3</sub> according to our eq. (8) (black), and also for including a correction for non-linear electron-phonon coupling (red). Experimental values are taken from Refs. [14, 41].

perconductivity, other mechanisms have also been discussed as potentially playing a role, such as the deformation potential mechanism [18, 46]. In order to evaluate the relevance of such mechanisms to electron pairing in SrTiO<sub>3</sub>, and due to the lack of analytic expressions for such electron-phonon interactions, we return to eq. (3) and evaluate this term from first principles including only short-range electron-phonon coupling  $g_{ii\mathbf{q}\nu}^{\mathcal{S}}(\mathbf{R})$ . Details of our first-principles implementation of eq. (3) are given in our companion paper [25]. Briefly, we use Quantum Espresso for DFT calculations [47], and Wannier90 [48] to produce MLWFs used as a basis for the terms in eqs. (1) and (3). The resulting MLWFs describing the conduction states of SrTiO<sub>3</sub> resemble Ti *d* orbitals, and yield a Wannier-interpolated band structure in excellent agreement with DFT (Fig. 1). We use RESPACK to evaluate the electronic Coulomb repulsion according to eq. (1) for the subspace of the three conduction states, within the constrained random phase approximation (cRPA) [49]. We use EPW [50], BerkeleyGW [51] and Abinit [52], allowing us to compute the phonon-mediated electron interaction following eq. (3) within *GW* perturbation theory (GWPT) [53], which captures the effect of many-

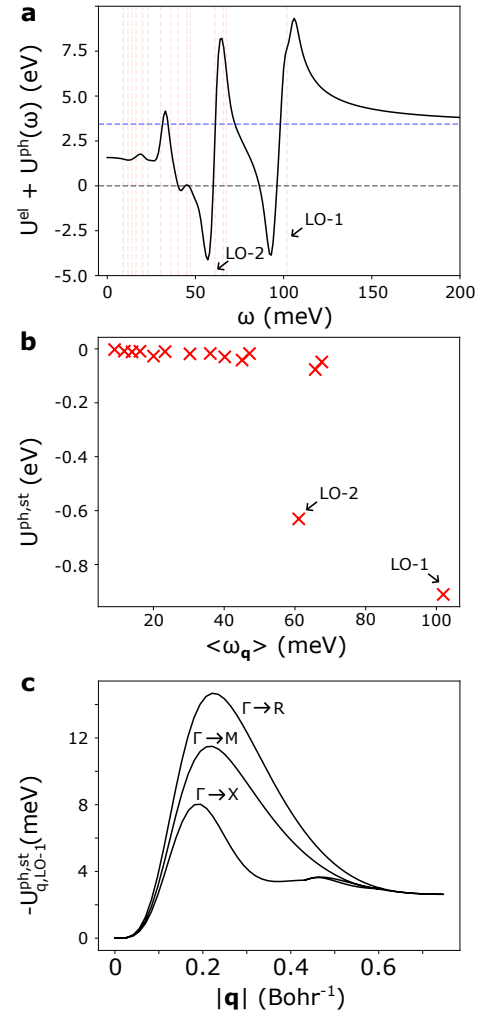


FIG. 3. On-site electron-electron interaction in SrTiO<sub>3</sub>, mediated by short-range coupling to phonons. In panel a we plot the frequency dependence of the total interaction, where red lines are average phonon frequencies in the Brillouin zone, and the blue dashed line marks the static purely electronic interaction. In panel b we decompose the static on-site attraction to the contributions of different phonons, and panel c shows how the contribution of LO-1 depends on its momentum  $|\mathbf{q}|$ .

electron correlations on the electron-phonon coupling.

The most important contribution of the phonon-mediated attraction due to short-range electron-phonon coupling is to the on-site ( $\mathbf{R} = \mathbf{R}'$ ) Coulomb term, where an attraction of  $U_{\mathbf{R}\mathbf{R}}^{\text{ph},st,\mathcal{S}} = -1.858 \text{ eV}$  is found. Within cRPA we find that the on-site repulsion between two conduction electrons is  $U_{\mathbf{R}\mathbf{R}}^{\text{el},st} = 3.436 \text{ eV}$ . Therefore, while there is a substantial reduction of 54% in the on-site Coulomb repulsion due to phonons, the overall interaction remains repulsive. To better understand the attractive contribution from short-range electron-phonon coupling, we visualize in Fig. 3a the frequency dependence of the total on-site electron-electron interaction, including phonon effects. Here we have applied a Gaussian smoothing filter to reduce noise. We see that there are

poles associated with the LO phonons, and it is only at fairly large frequencies of approximately 50 meV that the overall on-site interaction becomes attractive. While the static long-range phonon-mediated interaction between electrons is already sufficient to yield superconductivity, it is worth noting that this on-site interaction, which only becomes attractive at finite frequencies, could also contribute to superconductivity, as it has been shown in Hubbard-Holstein models with appropriate retardation and on-site interaction strength [54]. In Fig. 3b we visualize the contribution of individual phonons to the on-site phonon-mediated attraction in the static limit. This effect is dominated by the two highest frequency LO modes and we decompose the contribution of the highest frequency one (LO-1) along three high-symmetry paths in the Brillouin zone in Fig. 3c. We see that the absolute value of the phonon-mediated attraction initially grows with  $|\mathbf{q}|$ , and eventually peaks. This is consistent with analytic theories of electron-phonon coupling [31, 55], where the deformation potential includes octopole and higher-order terms, which vanish as  $\mathbf{q} \rightarrow 0$ .

It is worth asking what makes  $\text{SrTiO}_3$  special in terms of the emergence of attractive electron-electron interactions, and whether similar behavior might be observed in other materials. As presented above, there are two mechanisms for phonon-mediated attraction at play. The first is the long-range coupling of electrons to multiple LO phonons. As expressed by eq. (6), this channel is significant in materials where multiple LO phonons have a substantial splitting from the corresponding TO phonons - a manifestation of large Born effective charges. The second contribution to a strong phonon-mediated electron attraction is the deformation potential mechanism, which is generally associated with strong covalent character of the bonds of a material [56]. As seen in Table I the Born effective charges of the Ti and O values are much greater than their nominal charges, reflecting the ionic-covalent character of the Ti-O bond, similar to other cubic perovskites [57]. A similar phonon-mediated attraction due to a deformation potential mechanism was found for GeTe in our companion paper [25]. Our results are consistent with the anomalous isotope effect of  $\text{SrTiO}_3$ , where superconductivity is enhanced upon substitution

of  $^{16}\text{O}$  by  $^{18}\text{O}$  [58]. Oxygen substitution reduces the frequency of the lowest TO mode [59], which in turn will increase the attraction between electrons mediated by the deformation potential mechanism, given the  $1/\omega_{\mathbf{q},\nu}$  dependence of the phonon-mediated attraction  $U^{ph}$ .

We have presented a theoretical framework for the phonon-mediated electron interactions of materials, and applied it to  $\text{SrTiO}_3$ . We have shown that long-range coupling of electrons to multiple LO phonons can result in superconductivity, in good agreement with experiments. Moreover, we have derived a simple criterion to determine whether this mechanism appears within a given material. It will be interesting moving forward to examine in more detail the importance of long-range electron-phonon coupling for inducing superconductivity, as has been previously discussed in the context of high-temperature superconductivity [60]. Furthermore, we have combined our theory with first-principles calculations, and found a strong short-range phonon-mediated attraction of electrons, following a deformation potential mechanism, which is expected to be strong in systems with mixed ionic-covalent bonding. We expect that our theoretical and computational framework will contribute towards a deeper understanding of phonon-mediated superconductivity in a wide range of materials.

The authors are thankful to Marvin L. Cohen for helpful and inspiring discussions. This material is based upon work supported by the U.S. Department of Energy, Office of Science, National Quantum Information Science Research Centers, Superconducting Quantum Materials and Systems Center (SQMS) under contract No. DE-AC02-07CH11359. We are grateful for support from NASA Ames Research Center. C. J. N. C. and M. R. F. acknowledge support from the UK Engineering and Physical Sciences Research Council (EPSRC). VV was supported by the National Science Foundation (NSF) CAREER award through grant No. DMR-1945098. This research used resources of the National Energy Research Scientific Computing Center, a DOE Office of Science User Facility supported by the Office of Science of the U.S. Department of Energy under Contract No. DE-AC02-05CH11231 using NERSC awards HEP-ERCAP0029167 and DDR-ERCAP0029710.

---

[1] M. L. Cohen, Superconductivity in many-valley semiconductors and in semimetals, *Phys. Rev.* **134**, A511 (1964).

[2] M. L. Cohen, The existence of a superconducting state in semiconductors, *Rev. Mod. Phys.* **36**, 240 (1964).

[3] J. F. Schooley, W. R. Hosler, and M. L. Cohen, Superconductivity in Semiconducting  $\text{SrTiO}_3$ , *Phys. Rev. Lett.* **12**, 474 (1964).

[4] M. Kriener, M. Sakano, M. Kamitani, M. S. Bahramy, R. Yukawa, K. Horiba, H. Kumigashira, K. Ishizaka, Y. Tokura, and Y. Taguchi, Evolution of Electronic States and Emergence of Superconductivity in the Polar Semiconductor GeTe by Doping Valence-Skipping In- dium, *Phys. Rev. Lett.* **124**, 047002 (2020).

[5] H. Cheng, H. Yao, Y. Xu, J. Jiang, Y. Yang, J. Wang, X. Li, Y. Li, and J. Shao, Pressure-Induced Alloying and Superconductivity in GeTe, *Chemistry of Materials* **36**, 3764 (2024).

[6] P. B. Allen and M. L. Cohen, Carrier-concentration-dependent superconductivity in SnTe and GeTe, *Phys. Rev.* **177**, 704 (1969).

[7] M. Novak, S. Sasaki, M. Kriener, K. Segawa, and Y. Ando, Unusual nature of fully gapped superconductivity in In-doped SnTe, *Phys. Rev. B* **88**, 140502 (2013).

[8] J. M. Lu, O. Zheliuk, I. Leermakers, N. F. Q. Yuan,

U. Zeitler, K. T. Law, and J. T. Ye, Evidence for two-dimensional Ising superconductivity in gated MoS<sub>2</sub>, *Science* **350**, 1353 (2015).

[9] S. Gariglio, N. Reyren, A. D. Caviglia, and J.-M. Triscone, Superconductivity at the LaAlO<sub>3</sub>/SrTiO<sub>3</sub> interface, *Journal of Physics: Condensed Matter* **21**, 164213 (2009).

[10] J. Biscaras, N. Bergeal, A. Kushwaha, T. Wolf, A. Rastogi, R. C. Budhani, and J. Lesueur, Two-dimensional superconductivity at a Mott insulator/band insulator interface LaTiO<sub>3</sub>/SrTiO<sub>3</sub>, *Nature Communications* **1**, 10.1038/ncomms1084 (2010), [arXiv:1002.3737](https://arxiv.org/abs/1002.3737).

[11] S. Tan, Y. Zhang, M. Xia, Z. Ye, F. Chen, X. Xie, R. Peng, D. Xu, Q. Fan, H. Xu, J. Jiang, T. Zhang, X. Lai, T. Xiang, J. Hu, B. Xie, and D. Feng, Interface-induced superconductivity and strain-dependent spin density waves in FeSe/SrTiO<sub>3</sub> thin films, *Nature Materials* **12**, 634 (2013), [arXiv:1301.2748](https://arxiv.org/abs/1301.2748).

[12] J.-J. Zhou, O. Hellman, and M. Bernardi, Electron-Phonon Scattering in the Presence of Soft Modes and Electron Mobility in SrTiO<sub>3</sub> Perovskite from First Principles, *Phys. Rev. Lett.* **121**, 226603 (2018).

[13] G. Antonius, Y.-H. Chan, and S. G. Louie, Polaron spectral properties in doped ZnO and SrTiO<sub>3</sub> from first principles, *Phys. Rev. Res.* **2**, 043296 (2020).

[14] C. S. Koonce, M. L. Cohen, J. F. Schooley, W. R. Hosler, and E. R. Pfeiffer, Superconducting Transition Temperatures of Semiconducting SrTiO<sub>3</sub>, *Phys. Rev.* **163**, 380 (1967).

[15] L. P. Gor'kov, Phonon mechanism in the most dilute superconductor n-type SrTiO<sub>3</sub>, *Proceedings of the National Academy of Sciences* **113**, 4646 (2016).

[16] L. P. Gor'kov, Back to Mechanisms of Superconductivity in Low-Doped Strontium Titanate, *Journal of Superconductivity and Novel Magnetism* **30**, 845 (2017).

[17] Z. Han, S. A. Kivelson, and P. A. Volkov, Quantum bipolaron superconductivity from quadratic electron-phonon coupling, *Phys. Rev. Lett.* **132**, 226001 (2024).

[18] P. Wölfle and A. V. Balatsky, Superconductivity at low density near a ferroelectric quantum critical point: Doped SrTiO<sub>3</sub>, *Phys. Rev. B* **98**, 104505 (2018).

[19] M. N. Gastiasoro, M. E. Temperini, P. Barone, and J. Lorenzana, Generalized rashba electron-phonon coupling and superconductivity in strontium titanate, *Phys. Rev. Res.* **5**, 023177 (2023).

[20] C. Setty, M. Baggio, and A. Zaccone, Superconducting dome in ferroelectric-type materials from soft mode instability, *Phys. Rev. B* **105**, L020506 (2022).

[21] S. K. Saha, M. N. Gastiasoro, J. Ruhman, and A. Klein, *Strong Coupling Theory of Superconductivity and Ferroelectric Quantum Criticality in metallic SrTiO<sub>3</sub>* (2024), [arXiv:2412.05374 \[cond-mat.str-el\]](https://arxiv.org/abs/2412.05374).

[22] C. Collignon, X. Lin, C. W. Rischau, B. Fauqué, and K. Behnia, Metallicity and Superconductivity in Doped Strontium Titanate, *Annual Review of Condensed Matter Physics* **10**, 25 (2019).

[23] M. N. Gastiasoro, J. Ruhman, and R. M. Fernandes, Superconductivity in dilute SrTiO<sub>3</sub>: A review, *Annals of Physics* **417**, 168107 (2020).

[24] E. R. Margine and F. Giustino, Anisotropic migdal-eliashberg theory using wannier functions, *Phys. Rev. B* **87**, 024505 (2013).

[25] N. M. Tubman, C. J. N. Coveney, C.-E. Hsu, A. Montoya-Castillo, M. R. Filip, J. B. Neaton, Z. Li, V. Vlcek, and A. M. Alvertis, Theory of ab initio downfolding with arbitrary range electron-phonon coupling (2025), [arXiv:2502.00103 \[cond-mat.mtrl-sci\]](https://arxiv.org/abs/2502.00103).

[26] N. Marzari, A. A. Mostofi, J. R. Yates, I. Souza, and D. Vanderbilt, Maximally localized wannier functions: Theory and applications, *Rev. Mod. Phys.* **84**, 1419 (2012).

[27] G. Baym, Field-theoretic approach to the properties of the solid state, *Annals of Physics* **14**, 10.1006/aphy.2000.6009 (1961).

[28] L. Hedin, New Method for Calculating the One-Particle Green's Function with Application to the Electron-Gas Problem, *Physical Review* **139**, 796 (1965).

[29] F. Giustino, Electron-phonon interactions from first principles, *Reviews of Modern Physics* **89**, 1 (2017).

[30] G. D. Mahan, *Many-Particle Physics*, Physics of Solids and Liquids (Springer, 2013).

[31] P. Vogl, Microscopic theory of electron-phonon interaction in insulators or semiconductors, *Phys. Rev. B* **13**, 694 (1976).

[32] C. Verdi and F. Giustino, Fröhlich electron-phonon vertex from first principles, *Physical Review Letters* **115**, 1 (2015), [1510.06373](https://arxiv.org/abs/1510.06373).

[33] O. V. Dolgov, D. A. Kirzhnits, and E. G. Maksimov, On an admissible sign of the static dielectric function of matter, *Rev. Mod. Phys.* **53**, 81 (1981).

[34] A. Spinelli, M. A. Torija, C. Liu, C. Jan, and C. Leighton, Electronic transport in doped srtio<sub>3</sub>: Conduction mechanisms and potential applications, *Phys. Rev. B* **81**, 155110 (2010).

[35] Q. Ren, C. Fu, Q. Qiu, S. Dai, Z. Liu, T. Masuda, S. Asai, M. Hagiwala, S. Lee, S. Torri, T. Kamiyama, L. He, X. Tong, C. Felser, D. J. Singh, T. Zhu, J. Yang, and J. Ma, Establishing the carrier scattering phase diagram for zrnism-based half-heusler thermoelectric materials, *Nature Communications* **11**, 3142 (2020).

[36] F. Macheda, P. Barone, and F. Mauri, Electron-phonon interaction and longitudinal-transverse phonon splitting in doped semiconductors, *Phys. Rev. Lett.* **129**, 185902 (2022).

[37] R. Cowley, W. Buyers, and G. Dolling, Relationship of normal modes of vibration of strontium titanate and its antiferroelectric phase transition at 110°k, *Solid State Communications* **7**, 181 (1969).

[38] Y. Yamada and G. Shirane, Neutron Scattering and Nature of the Soft Optical Phonon in SrTiO<sub>3</sub>, *Journal of the Physical Society of Japan* **26**, 396 (1969), <https://doi.org/10.1143/JPSJ.26.396>.

[39] M. Zacharias, G. Volonakis, F. Giustino, and J. Even, Anharmonic lattice dynamics via the special displacement method, *Phys. Rev. B* **108**, 035155 (2023).

[40] Y. Zhang, J. Sun, J. P. Perdew, and X. Wu, Comparative first-principles studies of prototypical ferroelectric materials by LDA, GGA, and SCAN meta-GGA, *Physical Review B* **96**, 1 (2017).

[41] C. W. Rischau, X. Lin, C. P. Grams, D. Finck, S. Harms, J. Engelmayr, T. Lorenz, Y. Gallais, B. Fauqué, J. Hemberger, and K. Behnia, A ferroelectric quantum phase transition inside the superconducting dome of sr1-xcaxtio3- $\delta$ , *Nature Physics* **13**, 643 (2017).

[42] M. Zacharias, M. Scheffler, and C. Carbogno, Fully anharmonic nonperturbative theory of vibronically renormalized electronic band structures, *Phys. Rev. B* **102**, 045126 (2020).

[43] D. van der Marel, F. Barantani, and C. W. Rischau, Possible mechanism for superconductivity in doped  $\text{SrTiO}_3$ , *Phys. Rev. Res.* **1**, 013003 (2019).

[44] D. E. Kiselov and M. V. Feigel'man, Theory of superconductivity due to ngai's mechanism in lightly doped  $\text{SrTiO}_3$ , *Phys. Rev. B* **104**, L220506 (2021).

[45] P. A. Volkov, P. Chandra, and P. Coleman, Superconductivity from energy fluctuations in dilute quantum critical polar metals, *Nature Communications* **13**, 4599 (2022).

[46] J. Ruhman and P. A. Lee, Comment on "Superconductivity at low density near a ferroelectric quantum critical point: Doped  $\text{SrTiO}_3$ ", *Phys. Rev. B* **100**, 226501 (2019).

[47] P. Giannozzi, S. Baroni, N. Bonini, M. Calandra, R. Car, C. Cavazzoni, D. Ceresoli, G. L. Chiarotti, M. Cococcioni, I. Dabo, A. Dal Corso, S. Fabris, G. Fratesi, S. de Gironcoli, R. Gebauer, U. Gerstmann, C. Gougaussis, A. Kokalj, M. Lazzeri, L. Martin-Samos, N. Marzari, F. Mauri, R. Mazzarello, S. Paolini, A. Pasquarello, L. Paulatto, C. Sbraccia, S. Scandolo, G. Sclauzero, A. P. Seitsonen, A. Smogunov, P. Umari, and R. M. Wentzcovitch, QUANTUM ESPRESSO: a modular and open-source software project for quantum simulations of materials, *Journal of Physics: Condensed Matter* **21**, 395502 (2009).

[48] G. Pizzi, V. Vitale, R. Arita, S. Blügel, F. Freimuth, G. Géranton, M. Gibertini, D. Gresch, C. Johnson, T. Koretsune, J. Ibanez-Azpiroz, H. Lee, J. M. Lihm, D. Marchand, A. Marrazzo, Y. Mokrousov, J. I. Mustafa, Y. Nohara, Y. Nomura, L. Paulatto, S. Poncé, T. Ponweiser, J. Qiao, F. Thöle, S. S. Tsirkin, M. Wierzbowska, N. Marzari, D. Vanderbilt, I. Souza, A. A. Mostofi, and J. R. Yates, Wannier90 as a community code: New features and applications, *Journal of Physics Condensed Matter* **32**, 10.1088/1361-648X/ab51ff (2020).

[49] F. Aryasetiawan, M. Imada, A. Georges, G. Kotliar, S. Biermann, and A. I. Lichtenstein, Frequency-dependent local interactions and low-energy effective models from electronic structure calculations, *Phys. Rev. B* **70**, 195104 (2004).

[50] H. Lee, S. Poncé, K. Bushick, S. Hajinazar, J. Lafuente-Bartolome, J. Leveillee, C. Lian, J.-M. Lihm, F. Macheda, H. Mori, H. Paudyal, W. H. Sio, S. Tiwari, M. Zacharias, X. Zhang, N. Bonini, E. Kioupakis, E. R. Margine, and F. Giustino, Electron-phonon physics from first principles using the EPW code, *npj Computational Materials* **9**, 156 (2023).

[51] J. Deslippe, G. Samsonidze, D. A. Strubbe, M. Jain, M. L. Cohen, and S. G. Louie, BerkeleyGW: A massively parallel computer package for the calculation of the quasiparticle and optical properties of materials and nanostructures, *Computer Physics Communications* **183**, 1269 (2012), 1111.4429.

[52] X. Gonze, B. Amadon, G. Antonius, F. Arnardi, L. Baguet, J.-M. Beuken, J. Bieder, F. Bottin, J. Bouchet, E. Bousquet, N. Brouwer, F. Bruneval, G. Brunin, T. Cavignac, J.-B. Charraud, W. Chen, M. Côté, S. Cottenier, J. Denier, G. Geneste, P. Ghosez, M. Giantomassi, Y. Gillet, O. Gingras, D. R. Hamann, G. Hautier, X. He, N. Helbig, N. Holzwarth, Y. Jia, F. Jollet, W. Lafargue-Dit-Hauret, K. Lejaeghere, M. A. L. Marques, A. Martin, C. Martins, H. P. C. Miranda, F. Naccarato, K. Persson, G. Petretto, V. Planes, Y. Pouillon, S. Prokhorenko, F. Ricci, G.-M. Rignanese, A. H. Romero, M. M. Schmitt, M. Torrent, M. J. van Setten, B. Van Troeye, M. J. Verstraete, G. Zérah, and J. W. Zwanziger, The Abinit project: Impact, environment and recent developments, *Computer Physics Communications* **248**, 107042 (2020).

[53] Z. Li, G. Antonius, M. Wu, F. H. da Jornada, and S. G. Louie, Electron-Phonon Coupling from Ab Initio Linear-Response Theory within the  $GW$  Method: Correlation-Enhanced Interactions and Superconductivity in  $\text{Ba}_{1-x}\text{K}_x\text{BiO}_3$ , *Phys. Rev. Lett.* **122**, 186402 (2019).

[54] Z. Han, S. A. Kivelson, and H. Yao, Strong coupling limit of the holstein-hubbard model, *Phys. Rev. Lett.* **125**, 167001 (2020).

[55] P. Lawaetz, Long-wavelength phonon scattering in non-polar semiconductors, *Phys. Rev.* **183**, 730 (1969).

[56] M. L. Cohen and S. G. Louie, *Fundamentals of Condensed Matter Physics* (Cambridge University Press, 2016).

[57] W. Zhong, R. D. King-Smith, and D. Vanderbilt, Giant LO-TO splittings in perovskite ferroelectrics, *Phys. Rev. Lett.* **72**, 3618 (1994).

[58] A. Stucky, G. W. Scheerer, Z. Ren, D. Jaccard, J.-M. Poumirol, C. Barreteau, E. Giannini, and D. van der Marel, Isotope effect in superconducting n-doped  $\text{SrTiO}_3$ , *Scientific Reports* **6**, 37582 (2016).

[59] J. M. Edge, Y. Kedem, U. Aschauer, N. A. Spaldin, and A. V. Balatsky, Quantum Critical Origin of the Superconducting Dome in  $\text{SrTiO}_3$ , *Phys. Rev. Lett.* **115**, 247002 (2015).

[60] D.-H. Lee, Routes to high-temperature superconductivity: A lesson from fese/srtio3, *Annual Review of Condensed Matter Physics* **9**, 261 (2018).

[61] D. R. Hamann, Optimized norm-conserving Vanderbilt pseudopotentials, *Physical Review B - Condensed Matter and Materials Physics* **88**, 1 (2013), 1306.4707.

[62] M. J. van Setten, M. Giantomassi, E. Bousquet, M. J. Verstraete, D. R. Hamann, X. Gonze, and G. M. Rignanese, The PSEUDODOJO: Training and grading a 85 element optimized norm-conserving pseudopotential table, *Computer Physics Communications* **226**, 39 (2018), arXiv:1710.10138.

[63] B. Monserrat, Electron-phonon coupling from finite differences, *Journal of Physics: Condensed Matter* **30**, 083001 (2018).

[64] L. P. Gor'kov, Superconducting transition temperature: Interacting fermi gas and phonon mechanisms in the nonadiabatic regime, *Phys. Rev. B* **93**, 054517 (2016).

[65] B. Monserrat, Vibrational averages along thermal lines, *Phys. Rev. B* **93**, 014302 (2016).

[66] P. B. Allen and V. Heine, Theory of the temperature dependence of electronic band structures, *Journal of Physics C: Solid State Physics* **9**, 2305 (1976).

[67] P. B. Allen and M. Cardona, Theory of the temperature dependence of the direct gap of germanium, *Phys. Rev. B* **23**, 1495 (1981).

## Appendix A: Computational details

We employ Quantum Espresso [47] for DFT and DFPT calculations, Wannier90 [48] to generate Wannier states, and EPW [50] in order to perform Wannier-Fourier interpolation of electron-phonon matrix elements. We use scalar-relativistic optimized norm-conserving Vanderbilt pseudopotentials (ONCV) [61] with standard accuracy, taken from Pseudo Dojo [62]. We work within the local density approximation (LDA) of DFT. However, acoustic phonons obtained with DFPT become unstable at the  $R$  and  $M$  points of the Brillouin zone due to anharmonicity. To account for this anharmonicity, we displace the structure along an unstable harmonic phonon to find a new minimum in a supercell structure, and we re-compute the now stable phonons using finite differences [63], in a  $2 \times 2 \times 2$  supercell. For all DFT calculations we use a plane wave cutoff of 90 Ry. For crRPA calculations we compute the electronic density on a  $6 \times 6 \times 6$   $\Gamma$ -centered  $\mathbf{k}$ -grid, and we include 600 bands, using a cutoff of 20 Ry, and having excluded the three lowest-lying conduction bands. For DFPT and GWPT calculations we use an electronic density computed on a  $6 \times 6 \times 6$  half-shifted  $\mathbf{k}$ -grid, and we obtain the phonons on a  $6 \times 6 \times 6$  grid of  $\mathbf{q}$ -points ( $3 \times 3 \times 3$  for both grids for the  $2 \times 2 \times 2$  supercells). We interpolate the phonon frequencies and electron-phonon matrix elements on a  $20 \times 20 \times 20$   $\mathbf{q}$ -grid, which converges the short-range phonon-mediated attractive contribution to the Coulomb interactions within the conduction bands. It is worth highlighting that GWPT calculations are known to yield more accurate, and often stronger electron-phonon interactions compared to DFPT [53]. Indeed we found for SrTiO<sub>3</sub> that using GWPT increases the absolute value of the short-range on-site correction to the Coulomb interaction due to phonons by 18%, compared to DFPT.

## Appendix B: Cooper instability in Logarithmic approximation

SrTiO<sub>3</sub> becomes superconducting at very low doping densities, where  $\frac{\omega_\nu}{E_F} \gg 1$ , with  $\omega_\nu$  a typical phonon frequency. Following Gor'kov [15, 64], we take the logarithmic approach which is applicable in this non-adiabatic limit. Here superconductivity manifests itself in the emergence of a pole in the scattering amplitude of the dynamical screened Coulomb interaction as a result of the Dyson equation

$$\begin{aligned} \bar{U}_{\mathbf{kk}'}(i\omega_n) &= \tilde{U}_{\mathbf{kk}'}(i\omega_n) - \frac{T}{(2\pi)^3} \\ &\times \sum_m \int d\mathbf{k}_1 \tilde{U}_{\mathbf{kk}_1}(i\omega_n - i\omega_m) \\ &\times G_{\mathbf{k}_1}(i\omega_m) G_{-\mathbf{k}_1}(-i\omega_m) \bar{U}_{\mathbf{k}_1 \mathbf{k}'}(i\omega_m), \end{aligned} \quad (\text{B1})$$

where  $G$  the electron's Green's function. We obtain  $T_c$  from the eigenvalue of the homogeneous equation for the

gap function  $\Delta$ :

$$\begin{aligned} \Delta_{\mathbf{k}}(i\omega_n) &= -T \sum_m \int d\mathbf{k}_1 \tilde{U}_{\mathbf{kk}_1}(i\omega_n - i\omega_m) \\ &\times \Pi_{\mathbf{k}_1}(i\omega_m) \Delta_{\mathbf{k}_1}(i\omega_m), \end{aligned} \quad (\text{B2})$$

with the RPA polarization

$$\Pi_{\mathbf{k}}(i\omega_m) = G_{\mathbf{k}}(i\omega_m) G_{-\mathbf{k}}(-i\omega_m) = \frac{1}{\omega_m^2 + \left(\frac{k^2 - k_F^2}{2m^*}\right)^2}, \quad (\text{B3})$$

where we have made a parabolic band approximation. Solving for the gap function exactly gives  $T_c$  in a BCS weak-coupling form

$$T_c \propto \exp\left(-\frac{1}{\lambda}\right). \quad (\text{B4})$$

We now determine  $\lambda$  without solving the gap equation. Substituting the RPA polarization into the gap equation, we obtain

$$\begin{aligned} \Delta_{\mathbf{k}}(i\omega_n) &= -T \sum_m \int d\theta d\xi \tilde{U}_{\mathbf{kk}_1}(i\omega_n - i\omega_m) \frac{m^* p_F \sin \theta}{(2\pi)^2} \\ &\times \frac{1}{\omega_m^2 + \xi^2} \Delta_{\mathbf{k}_1}(i\omega_m). \end{aligned} \quad (\text{B5})$$

Let  $\mathbf{k}, \mathbf{k}_1$  be on the Fermi surface, (meaning  $|\mathbf{k}|^2 = |\mathbf{k}_1|^2 = |\mathbf{k}_F|^2$ ), and

$$\tilde{U}_{\mathbf{kk}_1}(i\omega_n - i\omega_m) \rightarrow \tilde{U}_{\mathbf{kk}_1}(0) = \frac{4\pi}{\epsilon_\infty} \cdot \frac{1 - \gamma^2}{|\mathbf{k} - \mathbf{k}_1|^2 + \kappa_{TF}^2}. \quad (\text{B6})$$

Given this form for the Coulomb interaction, the right-hand side of the gap equation eq. (B5) no longer depends on  $\omega_n$ , meaning that  $\Delta_{\mathbf{k}}(i\omega_n)$  must be a constant, and can be taken out of the integral. Therefore, we can devide both sides of the equation by  $\Delta_{\mathbf{k}}(i\omega_n)$ , and eq. (B5) simplifies to

$$\begin{aligned} 1 &= \left( \int_0^\pi d\theta \tilde{U}_{\mathbf{kk}_1}(\omega = 0) \frac{m^* p_F \sin \theta}{(2\pi)^2} \right) \\ &\times \int_0^W \frac{d\xi}{\xi} \tanh\left(\frac{\xi}{2T_c}\right), \end{aligned} \quad (\text{B7})$$

where  $W = A \cdot E_F$  the relevant energy scale, with  $A$  a constant of order unity. This may be rewritten as

$$1 = \lambda \ln\left(\frac{2W\gamma}{\pi T_c}\right), \quad (\text{B8})$$

from where we obtain

$$T_c = \frac{2W\gamma}{\pi} \exp\left(-\frac{1}{\lambda}\right). \quad (\text{B9})$$

The coupling constant  $\lambda$  is

$$\begin{aligned} \lambda &= \int_0^\pi d\theta \tilde{U}_{\mathbf{kk}_1}(\omega = 0) \frac{m^* p_F \sin \theta}{(2\pi)^2} \\ &= \frac{1 - \gamma^2}{2\pi\bar{\epsilon}_\infty} \int_0^\pi d\theta \frac{m^* \sin \theta}{p_F(1 - \cos \theta + \frac{\kappa_{TF}^2}{2p_F^2})}, \end{aligned} \quad (\text{B10})$$

and  $p_F^2 = 2m^* E_F$ . We evaluate the integral to obtain

$$\lambda = \frac{m^*(\gamma^2 - 1)}{2\pi p_F \bar{\epsilon}_\infty} \ln\left(1 + \frac{\pi p_F \bar{\epsilon}_\infty}{m^*}\right). \quad (\text{B11})$$

Now, we define the variable  $x = \pi p_F \bar{\epsilon}_\infty / m^*$  to get

$$\lambda = \frac{\gamma^2 - 1}{2x} \ln(1 + x). \quad (\text{B12})$$

By using this expression, substituting  $W$ , using the definition of the variable  $x$ , and given that  $2E_F = \frac{p_F^2}{m^*}$ , the critical temperature of eq. (B9) becomes

$$T_c = A \frac{m^* \gamma}{\pi^3 \bar{\epsilon}_\infty^2} x^2 \exp\left(-\frac{2x}{(\gamma^2 - 1) \ln(1 + x)}\right). \quad (\text{B13})$$

This expression reproduces the characteristic form of  $T_c$  as a function of charge carrier density.

### Appendix C: Impact of multi-phonon effects on the electron-phonon interaction

In order to evaluate the importance of higher-order electron-phonon coupling, we evaluate the coupling of conduction electrons to phonons using finite differences [63]. The vibrational average of the energy of the lowest conduction state  $E_{c\mathbf{k}}$ , at a given  $\mathbf{k}$ -point and temperature  $T$ , may be written as

$$E_{c\mathbf{k}}(T) = \frac{1}{Z} \sum_{\mathbf{s}} \langle \chi_{\mathbf{s}}(\mathbf{u}) | E_{c\mathbf{k}}(\mathbf{u}) | \chi_{\mathbf{s}}(\mathbf{u}) \rangle e^{-E_{\mathbf{s}}/k_B T}, \quad (\text{C1})$$

where  $\mathbf{u}$  a displaced nuclear configuration of the system,  $Z$  the partition function, and  $|\chi_{\mathbf{s}}(\mathbf{u})\rangle$  a vibrational eigenstate with energy  $E_{\mathbf{s}}$ . Equation (C1) includes electron-phonon interactions to all orders. We sample the integral of eq. (C1) using 100 thermal lines [65], which result to a narrow distribution around the average and correspond to displaced configurations based on the anharmonic phonons of SrTiO<sub>3</sub>. In Fig. 4 we visualize the shift of the lowest energy conduction state compared to the value without phonon effects, averaged over the Bril-

louin zone, *i.e.*,  $\Delta E = \frac{1}{N_k} \sum_{\mathbf{k}} (E_{c\mathbf{k}}(T) - E_{c\mathbf{k}}(\mathbf{u} = \mathbf{0}))$ , at  $T = 0, 100, 200, 300$  K.

We now expand  $E_{c\mathbf{k}}(\mathbf{u})$  in  $\mathbf{u}$ , truncate to second order, and write

$$\begin{aligned} &E_{c\mathbf{k}}(T) - E_{c\mathbf{k}}(\mathbf{u} = \mathbf{0}) \\ &= \sum_{\mathbf{q}, \nu} \frac{1}{2\omega_{\mathbf{q}, \nu}} \cdot \frac{\partial^2 E_{c\mathbf{k}}}{\partial u_{\mathbf{q}, \nu}^2} \left[ \frac{1}{2} + n_B(\omega_{\mathbf{q}, \nu}, T) \right]. \end{aligned} \quad (\text{C2})$$

This quadratic formula is the finite-difference equivalent of the Allen-Heine-Cardona theory for temperature-dependent band structures [66, 67], which is obtained from accounting for linear electron-phonon coupling, and where the correction is proportional to  $g^2$  ( $g$  is the electron-phonon matrix element). Therefore, differences in the values of  $E_{c\mathbf{k}}(T)$  when using eq. (C1) and eq. (C2) are due to higher-order coupling of conduction electrons to phonons, and in Fig. 4 we also plot the average correction to the conduction state energy across the Brillouin zone, as a function of temperature.

We find that while near  $T = 0$  K the two levels of theory are in good agreement, differences become more pronounced with increasing temperature, which is due to the more significant role of multi-phonon terms, as has been discussed in the literature [39, 42]. Nevertheless, the  $T = 0$  K limit is the relevant one for superconductivity in SrTiO<sub>3</sub>, and in this case we find that multi-phonon effects reduce the phonon-induced renormalization to 83% of its value when only considering linear coupling, across the Brillouin zone. We therefore estimate a similar reduction in the phonon-mediated attraction  $U^{ph} \propto g^2/\omega_\nu$ , once multi-phonon effects near  $T = 0$  K are accounted for, and as a correction we rescale  $g^2 \rightarrow 0.83g^2$ .

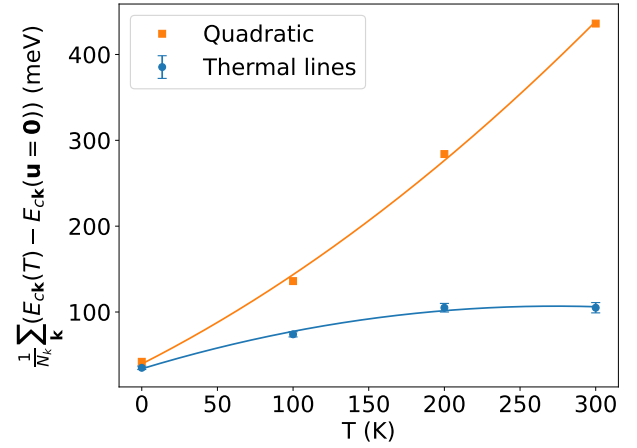


FIG. 4. Average renormalization of the SrTiO<sub>3</sub> conduction band energy across the Brillouin zone, as a function of temperature, using the thermal lines and quadratic methods.